JOURNAL OF APPLIED ELECTROCHEMISTRY 21 (1991) 1103–1113

Experimental and theoretical analysis of a thermogalvanic undivided flow cell with two aqueous electrolytes at different temperatures

J. M. HORNUT*‡, A. STORCK*

*Laboratoire des Sciences du Génie Chimique CNRS-ENSIC-INPL, BP. 451, 54001 Nancy, France
‡I.U.T. B. Université de Nancy I, Le Montet, 54600 Villers les Nancy, France

Received 3 March 1989; revised 6 March 1991

The electrochemical and thermal performance of a new thermogalvanic undivided flow cell using two aqueous electrolytes maintained at different temperatures between platinum electrodes is described. Measurements on the $Fe(CN)_6^{3-}/Fe(CN)_6^{4-}$ redox system in NaOH medium yield a thermoelectric effect between -1.1 and $-1.4\,mV/degree$ depending on the composition of the electrolytes. The influence of different parameters (temperature gradient, concentration of the electroactive species, fluid velocities and channel thickness) on the power output are determined. The experimental results show that electrical power is largely limited by charge and mass transfer overvoltages, but that it is possible to maintain the temperature gradient between the electrodes, i.e. the thermal boundary layers developing at the interface between the electrolytes do not reach the electrodes. A model based on the generalized Butler-Volmer kinetic equation is found to be in very good agreement with the experiments in terms of the current-voltage relationship and power output. This model is used for the prediction of the maximum electrochemical performance. From a practical point of view the efficiency of these devices remains very low due to the high thermal flux between the hot and cold electrolytes.

Nomenclature

C, C_A, C_B	molar concentrations ($mol\,m^{-3}$)
C_p	mass heat capacity ($J\,kg^{-1}\,K^{-1}$)
D	molecular diffusion coefficient ($m^2\,s^{-1}$)
d_h	hydraulic diameter of the cell (m)
E	equilibrium cell potential (V)
F	Faraday's constant = $96\,487\,C\,mol^{-1}$
I	cell intensity (A)
i	current density ($A\,m^{-2}$)
i_L	limiting current density ($A\,m^{-2}$)
i^*	dimensionless current density (defined in Equation 14)
i_0	exchange current density ($A\,m^{-2}$)
k_d	mass transfer coefficient ($m\,s^{-1}$)
L	length of channel (m)
P	electrical power (W)
p	specific electrical power ($W\,m^{-2}$)
Q_m	mass flowrate ($kg\,s^{-1}$)
R	external electrical resistance (Ω)
R_i	overall internal cell resistance (Ω or $\Omega\,m^2$)
R_m	membrane specific resistance ($\Omega\,m^2$)
R_i'	ohmic internal resistance (Ω or $\Omega\,m^2$)
Re	Reynolds number
Sh	Sherwood number
Sc	Schmidt number
t	time (s)
T	temperature (K)
u	mean fluid velocity ($m\,s^{-1}$)
U_c	cell voltage (V)
x	parameter defined in Equation 14
y	coordinate normal to electrode (m)

Greek symbols

α	electrochemical transfer coefficient (−)
Δ	half channel thickness (m)
ΔT	temperature difference ($T_C - T_f$) (K)
γ_e	number of electrons involved in the electrochemical reactions
η	overpotential (V)
Φ	thermal flux at the interface between the two flowing fluids (W)
ϕ	specific thermal flux ($W\,m^{-2}$)
λ	parameter defined in Equation 8 ($s^{-1/2}$)
γ	electrical conductivity ($\Omega^{-1}\,m^{-1}$)

Subscripts

A	relative to species A
a	at the anode
B	relative to species B
C	relative to the hot electrode (anode)
c	at the cathode
e	at the electrode
f	relative to the cold electrode (cathode)
opt	optimal
S	in the bulk

0021-891X/91 $03.00 + .12

1. Introduction

Galvanic thermopiles, or thermogalvanic cells, are electrochemical systems permitting the direct conversion of thermal energy into electrical energy [1] under the effect of a temperature gradient between two electrodes. In this system, the electrodes are brought to different temperatures and are in contact with a liquid or solid electrolyte. The thermoelectric effects at the electrodes give rise to an electromotive force [2, 3] which, since the electrodes are of the same nature, depends to a first approximation on the temperature gradient $(T_C - T_f)$ between the two electrodes and on the thermoelectric power, or non-isothermal temperature coefficient $(dE/dT)_{Th}$ of the reaction [4, 5]. Thermopiles can be classed in three categories:

(a) *Thermopiles with a molten salt electrolyte.* In this category, numerous examples were demonstrated during the 1960's [3, 5, 8]. In particular, Meissner [7] analyzed the influence of pressure on cell potential in the presence of different salts (LiBr, NaCl, AgCl) in the temperature region between the fusion point and 1300° C, while other workers [3, 6] have studied the theoretical available power.

(b) *Thermopiles with a solid electrolyte.* Reinhold [9, 10] was the first to address this type of galvanic cell from a thermodynamic viewpoint, but other sources describe further work in this area [11, 12]. The work of Wagner [11] concerns the thermoelectric power of solid electrolyte thermopiles, while Weininger [13] experimentally measured the discharge characteristics of the cells Ag|AgI|Ag and (Pt)I_2|AgI|I_2(Pt) for operating temperatures between 150 and 500° C. It follows from these various studies that: (i) the temperature coefficient is generally below 1.4 mV K^{-1} in the best case (for the system Cl_2|Ag|Cl_2), and (ii) the mass transfer phenomena at the electrodes seem to be the factors limiting the power of the thermopile.

(c) *Thermopiles with aqueous electrolyte.* For the case of cells with aqueous electrolyte, the experimental studies of thermopiles are the least numerous; one of the reasons being the limited operating temperature range available. The principal work on electrode phenomena for these systems was published by DeBethune *et al.* [2, 14, 15], who introduced two electrode coefficients: the first reflects the variation of the redox potential referenced to the hydrogen electrode with temperature (isothermal temperature coefficient), while the second corresponds to the contribution of the electrochemical reaction to the thermoelectric power of the redox couple utilized (nonisothermal temperature coefficient). Thermal migration phenomena in the electrolyte of galvanic cells was demonstrated by Agar [16] with the Ag^+/Ag couple. It appears that the value of the thermoelectric power depends only slightly on the nature of the cations in the liquid junction and remains relatively low (less than 0.55 mV K^{-1}). A thermodynamic treatment of the liquid junction phenomena was performed by Gaboriaud [17].

The utilization of thermogalvanic cells with aqueous electrolyte as a means of generating electricity has been the object of several articles and patents [18, 19], notably that of Clampitt [19] who studied a system functioning with the Cu^{2+}/Cu couple in sulphuric acid media. The performance obtained indicated a non-isothermal temperature coefficient of 1 mV K^{-1} and a maximum power of 2.5 W m^{-2}. Burrows [20, 21] described thermopiles based on the Fe^{2+}/Fe^{3+} couple in sulphuric media [20] and the $Fe(CN)_6^{3-}/Fe(CN)_6^{4-}$ couple in aqueous potassium sulphate [21]. The maximum power obtained with the latter couple, for which $(dE/dT)_{Th} = -1.48$ mV K^{-1}, was of the order of 5 W m^{-2} for a temperature gradient in the neighbourhood of 50° C. Generally, the creation of a galvanic thermopile with aqueous electrolyte must satisfy two requirements which are *a priori* contradictory: (i) minimization of the thermal short circuit between the two cell compartments, and (ii) minimization of all forms of overpotential at both electrodes in the cell (minimization of electrochemical and diffusional activation resistances) and the ohmic resistance.

The reduction of the interelectrode distance and the flow of electrolyte through the length of the electrode (in order to reduce diffusional limitations) constitute two favourable means for satisfying constraint (ii) above.

The original idea of circulating the electrolyte between two planar electrodes in order to limit the thermal short circuit between the compartments can be represented by the schematic diagram of Fig. 1.

This design is characterized by the existence of two distinct hydraulic circuits (one hot and one cold) circulating the length of each of the two electrodes which face one another. If the hydrodynamic regime is regular and well established, two thermal boundary layers develop in the contact plane of the two fluids. Under certain conditions, it is possible to maintain the electrodes at constant temperatures, T_C and T_f, respectively, and the thermal flux takes place at the interface of the two fluids. If the electrodes rest at constant temperatures, the electromotive force of the generator is thus a function of the temperature coefficient of the oxidation-reduction couple chosen and of the temperature gradient $\Delta T = T_C - T_f$.

$$E = (dE/dT)_{Th}(T_C - T_f) \qquad (1)$$

2. Apparatus, operating conditions and measurement techniques

This work concerns an experimental and theoretical analysis of the operation of a galvanic thermopile in aqueous medium operating according to the scheme in Fig. 1 and utilizing the redox couple $Fe(CN)_6^{3-}/Fe(CN)_6^{4-}$, for which the electrochemical kinetic characteristics and the temperature coefficient seem to be satisfactory. The specific interest of the study is the influence of the principal parameters (circulation rate, physicochemical properties of the fluids and cell thick-

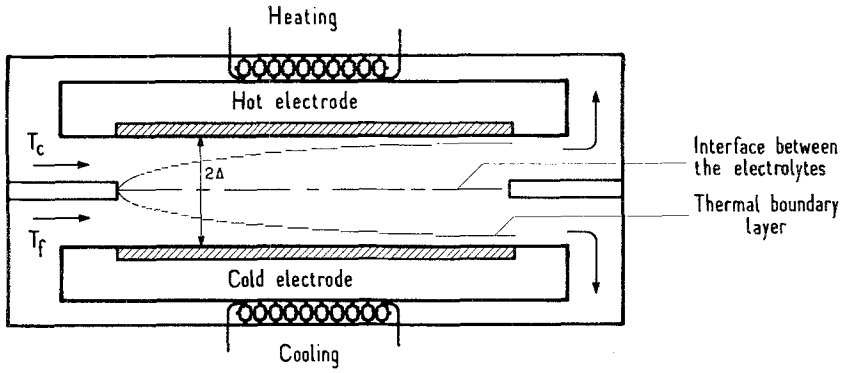

Fig. 1. Principle of the hydrodynamic system using two flowing electrolytes at different temperatures.

ness) on the electrical performance of the thermopile and the thermal flux at the interface of the two fluids.

2.1. *The electrochemical reactor*

The electrochemical reactor, represented in Fig. 2, is a rectangular cell with two planar electrodes and a perpendicular configuration (the direction of electric current flow is perpendicular to that of fluid flow). A stainless steel separator, formed by two 0.5 mm thick sheets mounted together, and containing a rectangular opening (140 mm × 150 mm) at the level of the electrodes, constitutes the middle part of the reactor. The edges of the opening perpendicular to the flow direction are bevelled to avoid introducing hydrodynamic perturbations at the contact plane between the two fluids. The reactor can eventually be equipped with a membrane, placed between the two stainless steel sheets, permitting the separation of the anodic and cathodic compartments. On each side of the separator, two Altuglass™ (methyl polymethylacrilate) spacers, having the same thickness, allow careful control of the interelectrode distance. The two symmetrical support plates A and B, which are also Altuglass™, and in which the electrodes are implanted, are placed against the electrodes and the entire assembly is held together with bolts along its perimeter. O-rings mounted within the cell assure a good seal. The cell is thermally isolated with 4 cm of ARMAFLEX™ insulating foam.

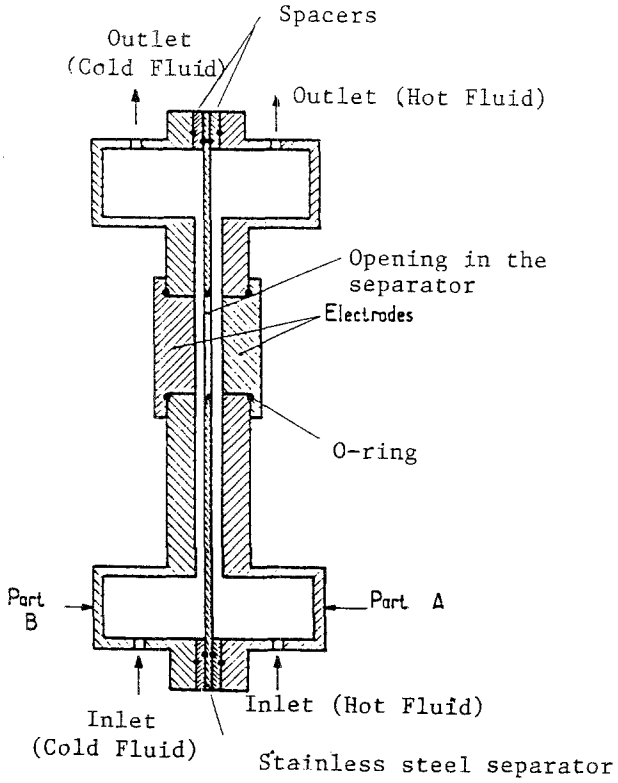

Fig. 2. Schematic view of the undivided thermogalvanic flow cell and associates equipment. 1, 2: cryothermostats; 3, 4: centrifugal pumps; 5, 6: valves; 7, 8: rotameters; and 9, 10: electrodes.

The platinized titanium (deposited by painting) electrodes are of the same dimensions and are held in place with screws, facing one another, in cell parts A and B.

2.2. *Fluid circulation*

The hot and cold fluids are stored in cryothermostatic baths and maintained at their assigned temperatures T_C and T_f. Circulation of the fluids is accomplished with centrifugal pumps; careful control and measurement of the flowrates are assured with valves and rotameters. The fluids flow through the cell at the same volumetric flowrate in each compartment, and the velocity is uniformly distributed through the use of calming zones in the base of the thermopile. In the absence of a membrane, the two fluids, both flowing in the laminar flow regime, and held respectively at T_C and T_f, come into contact at the level of the electrodes. The fluids are then separated after passing the electrodes and recycled to the two respective cryothermostatic baths for thermal regeneration.

2.3. *The solutions and their properties*

The galvanic thermopile realized here featured the $Fe(CN)_6^{3-}/Fe(CN)_6^{4-}$ redox couple in 1 M NaOH basic media. The solutions were prepared with Rhône Poulenc RP Normapure salts: $K_4Fe(CN)_6$, $3H_2O$ and $K_3Fe(CN)_6$, having a purity greater than 99%. The electrolyte solutions, which were prepared with the same concentration, were replaced regularly, to eliminate the effects of degradation by light [22] and consumption of the products. The exact concentration of potassium ferricyanide was determined with an amperometric method using a platinum rotating disc electrode in ammonia media containing a cobalt sulphate solution [29].

The physicochemical properties of the electrolytes (viscosity, density, electrical conductivity and diffusion coefficients) were determined experimentally; while the heat capacity and the thermal conductivity were estimated from literature values [23–28].

2.4. *Measurement techniques*

Prior to each experiment, the electrodes of the thermopile were electrochemically activated in a solution of 1 M NaOH. This activation consisted of several successive anodic and cathodic operations, each of several minutes duration, with hydrogen and oxygen evolution respectively.

Under steady state conditions, the open circuit potential of the cell, E, was experimentally determined with a Schlumberger digital voltmeter. The thermopile was then connected across a variable resistance, R. The potential, U_C, of the cell was then determined from the current, I, flowing in the circuit for various values of R.

The temperatures of the two fluids were measured with Chromel/Alumel thermocouples located at the entrance and exit of each of the two compartments. The knowledge of these two temperatures and the mass flowrates of the fluids in each compartment gives access to the heat flux exchanged at the interface, by use of the following relations:

$$\Phi = Q_{mC} C_{pC} \Delta T_C = Q_{mf} C_{pf} \Delta T_f \qquad (2)$$

3. Experimental results

3.1. *Determination of the nonisothermal temperature coefficients of the $Fe(CN)_6^{3-}/Fe(CN)_6^{4-}$ couple in NaOH media*

The apparatus shown in Fig. 3, which consisted of two perfectly mixed, doubly enveloped cells, each of 150 cm^3 volume, was used. Two cryothermostats (Huber T300) were utilized to impose the temperature of each cell. Ionic migration between the two compartments was assured by a salt bridge of the same nature as the solutions. The potential difference, E, was measured between two platinum wires submerged in the two solutions. Figure 4 shows the variation of open circuit potential, E, with temperature difference $(T_C - T_f)$ for various experimental conditions (concentrations of electrolyte and electroactive species). The perfect linearity of the data shows that the coefficient (dE/dT) is independent of the driving force $(T_C - T_f)$ in the region studied. Moreover, it appears that the increase in the ionic strength of the solution is the reason for the reduction in the absolute value of the temperature coefficient, which remains practically independent of the concentration of electroactive species $(Fe(CN)_6^{3-}/Fe(CN)_6^{4-})$ in the range considered. These results are in good agreement with theoretical calculations based on the thermodynamic principles of irreversible processes [30].

3.2. *Electrical performance of the galvanic thermopile in the absence of a separating membrane*

Figures 5 to 10 show the essential experimental results obtained in the form of potential-current (U_C against I) and available electric power-resistance (P against R) relations. The theoretical curves corresponding to each experiment were obtained by use of the treatment in section 4.3, which is based on kinetics.

3.2.1. Influence of the electrolyte circulation rate. For an interelectrode distance of 6 mm, an equal concentration of the oxidation-reduction couple of 0.2 M and a temperature difference $(T_C - T_f)$ of 20° C, Figs 5 and 6 show the influence of flowrate u of each fluid on the electrical performance of the thermopile.

The figures show that:

(i) the extrapolation of the U_C against I curves to zero

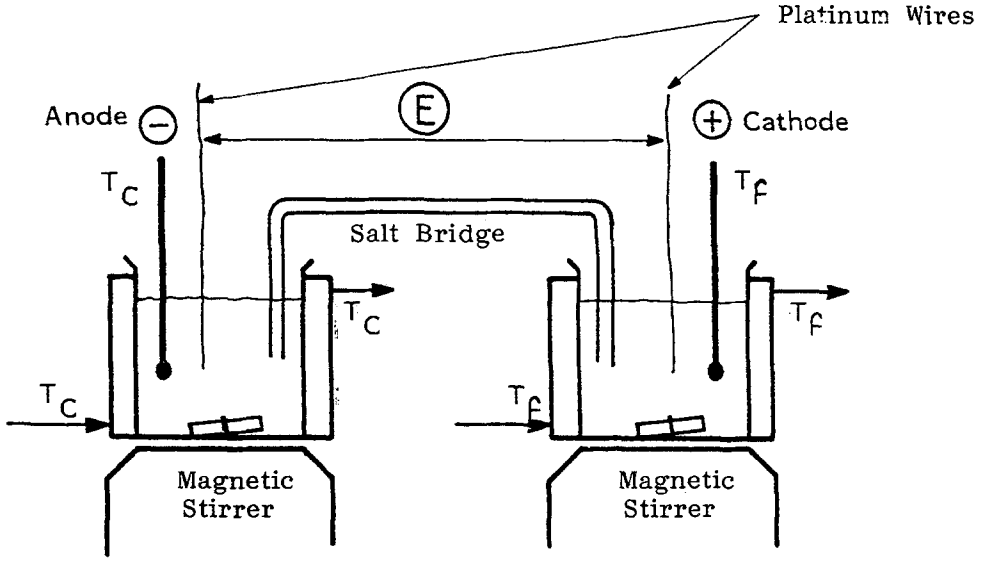

Fig. 3. Schematic view of the device used for the determination of the thermoelectric power $(dE/dT)_{th}$.

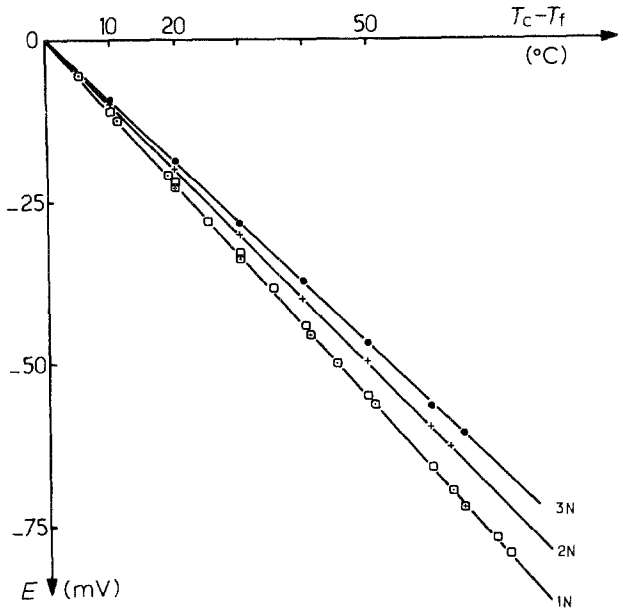

Fig. 4. Experimental variations of the electromotive force E with the temperature difference $\Delta T = T_c - T_f$ under different conditions: (□) 0.1, (⊡) 0.2, (⊞) 0.3 M, (+) NaOH = 2 N and (●) NaOH = 3 N for $[Fe(CN)_6^{4-}] = [Fe(CN)_6^{3-}] = 0.1$ M.

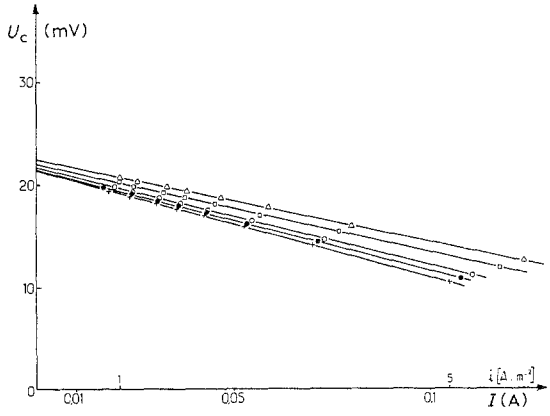

Fig. 5. Experimental variations of the cell voltage U_c with the current density. Influence of the electrolyte velocities, u: (+) 2.56×10^{-2}; (●) 3.156×10^{-2}; (○) 3.78×10^{-2}; (□) 5.05×10^{-2}; (△) 6.31×10^{-2} m s^{-1}. (——) Theoretical curve. Electrolyte concentration: $[Fe(CN)_6^{3-}] = [Fe(CN)_6^{4-}] = 0.2$ M. $2\Delta = 6 \times 10^{-3}$ m.

current gives a value of open circuit electromotive force, E, which is practically independent of the flowrate, and in perfect agreement with the value of the temperature coefficient of -1.1 mV deg C^{-1} determined independently (*cf.* Fig. 4). This result proves that, for these experimental conditions, the *thermal gradient is effectively maintained between the two electrodes along their entire length.*

(ii) the relationships $U_C = f(I)$ are linear and the global internal resistance, R_i (containing the contributions of activation overpotentials, diffusional limitations and ohmic resistance), can be considered as independent of the operating current. The value of R_i decreases as the flowrate u increases, probably due to a minimization of the concentration polarization phenomena at the level of the electrodes.

(iii) the power curves represent a maximum for a given value of the resistance of the external circuit, R_{opt}, which strongly depends on the flowrate u. In the case where the internal resistance, R_i, of the generator can be considered independent of the operating current I (*cf.* Fig. 5), the available electrical power P is given by

$$P = \frac{E^2}{R(1 + R_i/R)^2} \tag{3}$$

P is at its maximum value for $R_{opt} = R_i$ and

$$P_{opt} = E^2/4R_i \tag{4}$$

The experimental results of Fig. 6 are in perfect agreement with the theoretical expression in Equation 2, the values of R_i being determined from the slope in Fig. 5.

Table 1 shows other experimental results obtained for larger temperature gradients ($T_C - T_f$), up to 40° C. The optimal power is an increasing function of this gradient, which is in accord with Equation 4. This increase can be attributed to: (a) an increase in the open circuit potential, E, which is proportional to ($T_C - T_f$), and (b) a reduction in the global resistance, R_i, resulting from more rapid kinetics at the electrodes and a lower ohmic resistance under the effect of an increase in temperature T_C with respect to T_f. Further, the contribution of the electrolyte ohmic

Table 1.

Concentration (M)	$\Delta T = T_c - T_f$ (° C)	$\bar{u} \times 10^2$ ($m s^{-1}$)	*E (experimental)* (*mV*)	*E (theory)* (*mV*)	$R_i \times 10^3$ (Ωm^2)	$R_i' \times 10^4$ (Ωm^2)	$P_{opt} \times 10^2$ ($W m^{-2}$)
0.2	19.6	2.56	21.3	21.56	2.121	2.409	5.33
	19.7	3.156	21.4	21.67	2.058	2.409	5.56
	20.0	3.78	21.8	22.00	2.016	2.409	5.89
	20.1	5.05	22.0	22.11	1.806	2.409	6.69
	20.4	6.31	22.4	22.44	1.701	2.409	7.37
0.2	39.0	3.78	42.8	42.90	1.785	2.154	25.65
	39.1	5.05	43.1	43.01	1.68	2.154	27.64
	39.6	6.31	43.6	43.56	1.5855	2.154	29.97
	39.7	7.57	43.6	43.67	1.5015	2.154	31.65
	39.9	8.83	44.0	43.89	1.428	2.154	33.89

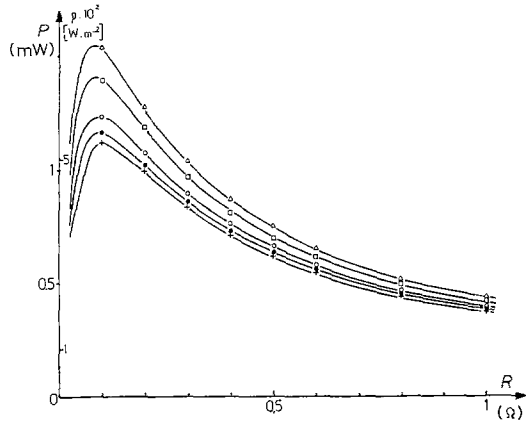

Fig. 6. Power output as a function of the output resistance, R. Influence of the electrolyte velocities (details as in Fig. 5).

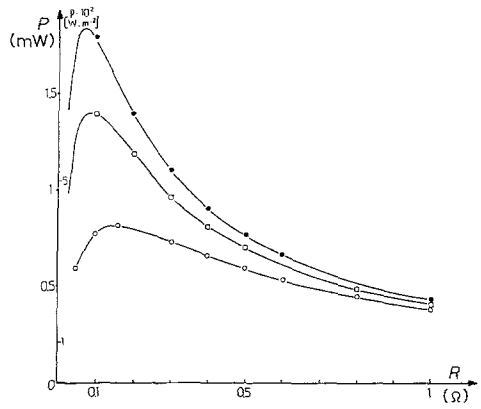

Fig. 8. Power output as a function of the output resistance, R. Influence of the concentrations of $Fe(CN)_6^{3-}$ and $Fe(CN)_6^{4-}$ (as in Fig. 7).

resistance, R_i', to the global resistance, R_i, is relatively small (of order 8 to 15%). This result illustrated the relative significance of overpotential resistances at the electrodes (diffusional and activation) with respect to ohmic effects.

3.2.2. Influence of molar concentration of the electroactive species. Figures 7 and 8 show the influence of the equal concentration in $Fe(CN)_6^{3-}$ and $Fe(CN)_6^{4-}$ ions on the electrical performance of the cell (for $T_C - T_f = 20°C$, $u = 5.05\,cm\,s^{-1}$ and an interelectrode distance of $2\Delta = 6\,mm$). Qualitatively, the same conclusions can be drawn as above, particularly with respect to the linearity of the U_C against I results, the value of the open circuit electromotive force, E, and the good agreement of the power results with Equation 2. From a quantitative viewpoint, the global internal resistance, R_i, is strongly dependent on the molar concentration of the electroactive species, C (also see the second part of Table 1), and noticeably decreases as C increases. This reduction may be attributed to activation and concentration overpotentials (see section 4) at the electrodes.

3.2.3. Influence of the interelectrode distance, 2Δ. The influence of this parameter, which varies between 6 and 14 mm, is shown in Figs 9 and 10, as well as in the last part of Table 1. The increase in 2Δ leads to a marked increase in R_i and thus to a decrease in the available electrical power, in agreement with Equation 3. This slight increase in R_i can be explained by the small contribution of the ohmic resistance R_i' to the total resistance R_i. The results in Fig. 11 quantitatively confirm this interpretation, the difference $(R_i - R_i')$ attributable to activation and concentration overpotential resistances being independent of the channel thickness, all other things being equal.

3.3. *Thermal performance of the galvanic thermopile in the absence of a separating membrane*

Figure 12 presents the experimental variation in the thermal flux at the interface between the two fluids with flowrate, u, for different temperature gradients and electroactive species concentration. The increase in the flowrate results in an increase in the thermal flux, Φ, due to the concommitant effects of hydrodynamic perturbation at the interface. With regard to the influence of the other major parameters, the results obtained show that: (i) Φ increases with the difference $(T_C - T_f)$; (ii) Φ decreases as the equiconcentration of species, C, increases; a result of the increase in

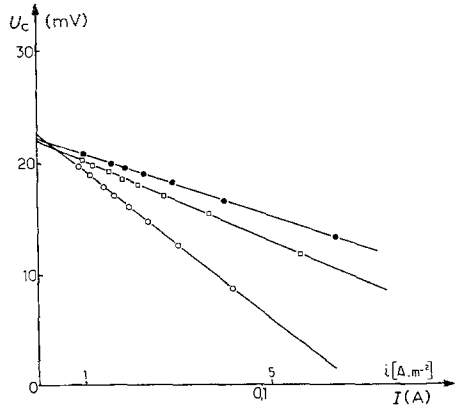

Fig. 7. Experimental variations of the cell voltage U_c with the current. Influence of the concentrations: $[Fe(CN)_6^{3-}] = [Fe(CN)_6^{4-}]$: (○) 0.1, (□) 0.2 and (●) 0.3 M. (——) Theoretical curve.

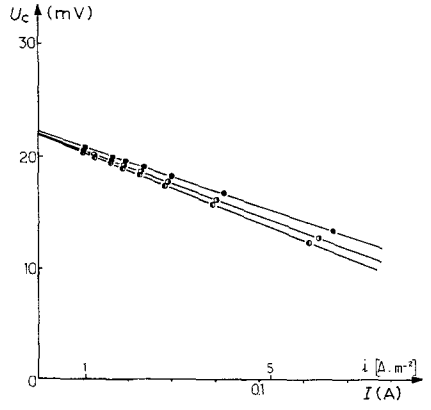

Fig. 9. Experimental variations of the cell voltage U_c with the current density. Influence of the channel thickness 2Δ: (●) 6, (◐) 10 and (◐) 14 mm. Electrolyte concentration: $[Fe(CN)_6^{3-}] = [Fe(CN)_6^{4-}] = 0.3\,M$. Electrolyte speed, $u = 5.05\,cm\,s^{-1}$. (——) Theoretical curve.

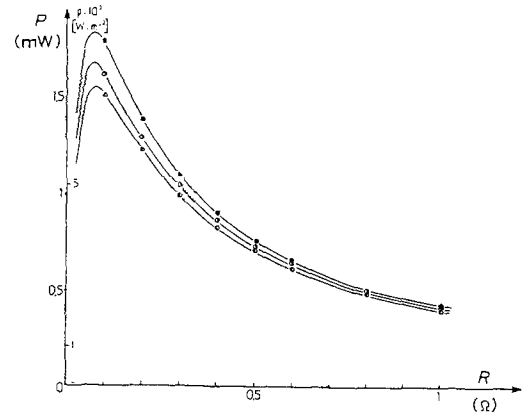

Fig. 10. Power output as a function of the output resistance, R. Influence of the channel thickness 2Δ. Details as in Fig. 9.

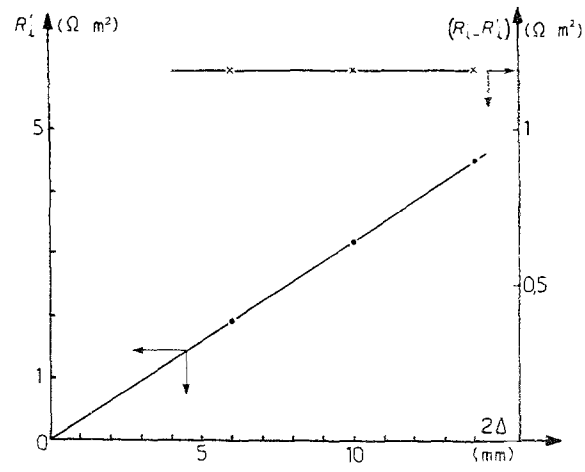

Fig. 11. Variations of the calculated ohmic resistance R_i' and the difference $(R_i - R_i')$ with the channel thickness 2Δ. Conditions: $u = 5.05 \times 10^{-2}$ cm s^{-1}; $T_c - T_f = 20°C$; both electrolyte concentrations = 0.3 M.

the dynamic viscosity of the fluids which favours a minimization of the interfacial hydrodynamic perturbations; and (iii) Φ increases with the channel thickness 2Δ for a given liquid flowrate.

A model based on the existence of an interfacial mixing zone (the depth of which depends on the Reynolds number) and the development of two thermal boundary layers at either side of this zone represents the experimental heat transfer results very well [30]. The values of flux Φ are relatively large with respect to the limited electrical performance obtained experimentally.

3.4. *Electrical and thermal performance of the generator equipped with a separating membrane*

In order to minimize Φ, a water-permeable cellophane membrane was placed between the two compartments of the cell. The electrical performance of the divided cell is shown in Figs 13 and 14, which indicate that the global internal resistance, R_i, is little affected by the presence of the separator. This is equally true for the electrical power delivered (decreased by 8%).

A comparison of the values of R_i with and without the separator, but otherwise under identical operating conditions permits an estimation of the membrane specific resistance, R_m, which was found to be approximately $1.4 \times 10^{-4}\ \Omega m^2$. The value of the heat flux, Φ is considerably reduced in the presence of the membrane, as shown in Fig. 12. Thus, the global yield, defined as the amount of electrical energy produced in comparison to the amount of thermal energy exchanged between the two fluids in contact, was found to have changed considerably.

The use of a separating membrane thus constitutes an efficient means of augmenting the global yield of the thermopile.

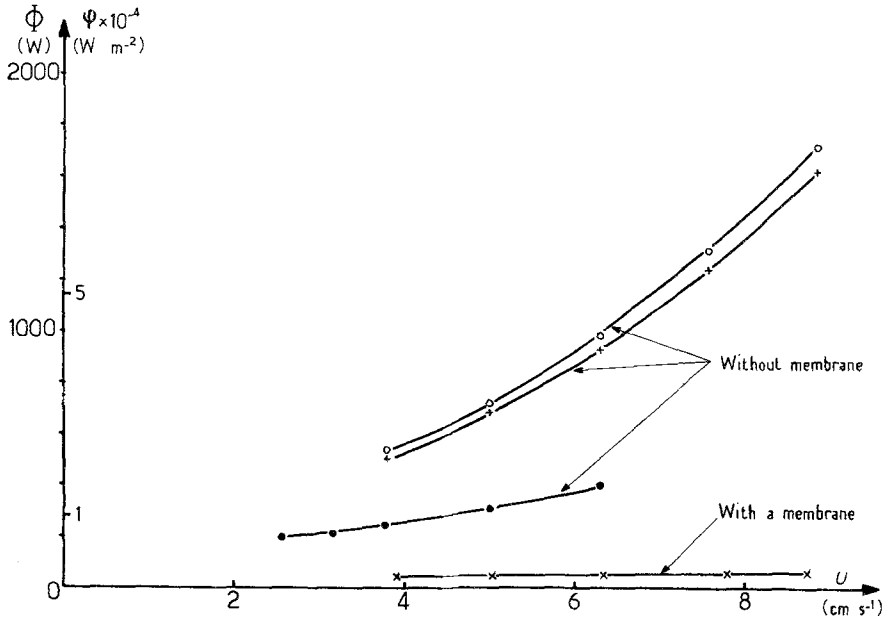

Fig. 12. Influence of the electrolyte velocities on the thermal flux at the interface between the two electrolytes. Conditions: $2\Delta = 6$ mm; [NaOH] = 1 N. Both electrolyte concentrations: (●) 0.2 M at $\Delta T = 20°C$, (+) 0.2 M at $\Delta T \simeq 39.5°C$, (○) 0.1 M at $\Delta T \simeq 39.5°C$, and (×) 0.2 M at $\Delta T = 20°C$.

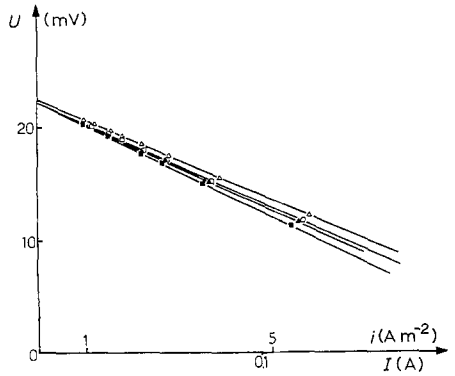

Fig. 13. Influence of the presence of a membrane on the current-voltage curves. Both concentrations: 0.2 M; $\Delta T = 20°$ C. Electrolyte speeds: (□) 5.05 (without membrane), (■) 5.05 (with membrane), (△) 6.31 (without membrane), and (▲) 6.31 cm s^{-1} (with membrane).

4. Theoretical analysis of the electrical behaviour of the generator

The interpretation of the electrochemical performance of the generator was carried out on the basis of the following hypotheses: (i) the operating conditions are such that the thermal boundary layers do not reach the electrodes, which are therefore maintained at T_C and T_f, respectively; (ii) the reaction kinetics at the anode and cathode can be represented by generalized Butler-Volmer relations, taking into account concentration polarization phenomena; (iii) diffusional limitations are evaluated with a Nernst film model; and (iv) the physicochemical properties of the fluids are calculated at the average temperature of each of the two electrolytes.

Under these conditions, the Butler-Volmer equation applied to the anode (hot electrode) is

$$i = i_{oa}\{(C_{Be}/C_{BS}) \exp [\alpha(\gamma_e F/RT)\eta_a] - (C_{Ae}/C_{AS}) \exp [-(1 - \alpha)(\gamma_e F/RT)\eta_a]\} \quad (5)$$

and the concentrations at the electrode (subscript e) or in the bulk solution (subscript S) are related by the global mass transfer coefficient, k_{da}, by

$$\left.\begin{aligned} C_{Ae} &= C_{AS} + \frac{i}{\gamma_e F k_{da}} \\ C_{Be} &= C_{BS} - \frac{i}{\gamma_e F k_{da}} \frac{D_A}{D_B} \end{aligned}\right\} \quad (6)$$

where $k_{da} = D_A/\delta$.

Combination of Equations 5 and 6 gives the global kinetic equation:

$$i = i_{oa}\{\exp [\alpha(\gamma_e F/RT)\eta_a] - \exp [-(1 - \alpha)(\gamma_e F/RT)\eta_a]\} \times \left[1 + i_{oa}\left\{\frac{D_A}{D_B}\frac{\exp [\alpha(\gamma_e F/RT)\eta_a]}{\gamma_e F k_{da} C_{BS}} + \frac{\exp [-(1 - \alpha)(\gamma_e F/RT)\eta_a]}{\gamma_e F k_{da} C_{AS}}\right\}\right]^{-1} \quad (7)$$

An identical expression can be written for the cathode (cold electrode), which relates the cathodic overpotential, η_C, to the operating current density, i.

The relationship between the electromotive force, U_C, of the generator and i can be deduced from the following:

$$U_C = E - \eta_a(i) - |\eta_c(i)| - R_i' i \quad (8)$$

where the overpotentials η_a and η_c are calculated at temperatures T_C and T_f, respectively with Equation 7, and the specific ohmic resistance, R_i', of each compartment at its average temperature. In the case where the generator is equipped with a separating membrane, a supplementary term $-R_m i$ representing the contribution of the membrane should be added to the right hand side of Equation 8.

4.1. *Experimental determination of electrochemical kinetic parameters of the* $Fe(CN)_6^{3-}/Fe(CN)_6^{4-}$ *couple*

The principle of Vetter's method [31] is based on the transient current response of an electrode, in static media, which is subjected to a step overpotential η from thermodynamic equilibrium. For a reaction of the type $A + \nu_e e^- \rightarrow B$ which follows the generalized Butler-Volmer Equation 5, the resolution of the diffusion equation in static medium yields the following transient expression [31]:

$$i(t) = i(0) \exp (\lambda^2 t) \operatorname{erfc} (\lambda\sqrt{(t)}) \quad (9)$$

with

$$\lambda = (i_0/\gamma_e F)\{(C_{BS}\sqrt{D_B})^{-1} \exp [\alpha(\gamma_e F/RT)\eta] + (C_{AS}\sqrt{D_A})^{-1} \exp [-(1 - \alpha)(\gamma_e F/RT)\eta]\}$$

For $t = 0$:

$$i(0) = i_0 \{\exp [\alpha(\gamma_e F/RT)\eta) - \exp [-(1 - \alpha)(\gamma_e F/RT)\eta]\} \quad (10)$$

and for $\lambda\sqrt{t} \ll 1$, Equation 9 is reduced to:

$$i(t) = i(0)\{1 - (2/\pi^{1/2})\lambda t^{1/2}\} \quad (11)$$

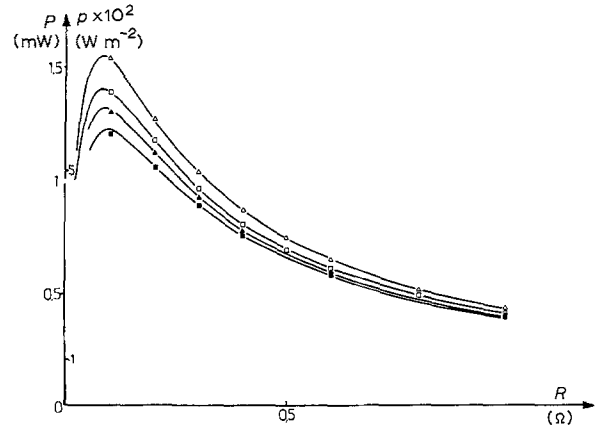

Fig. 14. Influence of the presence of a membrane on the power output. Details as in Fig. 13.

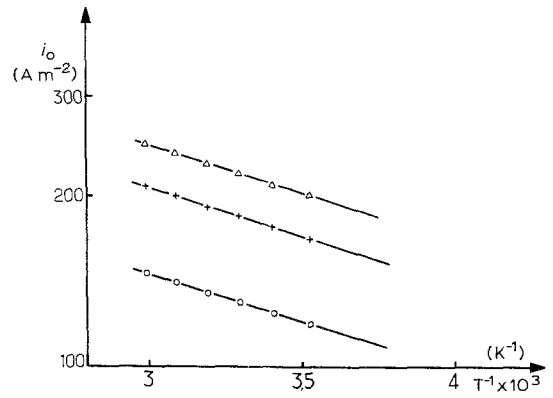

Fig. 15. Experimental results for electrochemical kinetic parameters determined by a transient technique. Both electrolyte concentrations: (○) 0.1, (+) 0.2 and (△) 0.3 M.

The two Relations 10 and 11, were used to determine the values of the exchange current density, i_0, and the symmetry factor, α, under various experimental conditions of temperature and concentration of the electroactive species. The results of the experimental analysis, obtained with a thermostated three electrode cell [30] are in perfect accord with the theoretical prediction of Relation 11, except for concentrated solutions where basic diffusion equations of the type $\partial C/\partial t = D(\partial^2 C/\partial y^2)$ are no longer applicable.

Figure 15 furnishes several examples of results concerning i_0, the average value of α obtained was 0.49, in good agreement with the literature.

4.2. *Experimental determination of physical kinetic parameters of the $Fe(CN)_6^{3-}/Fe(CN)_6^{4-}$ couple*

The mass transfer coefficients k_{da} and k_{dc} were determined experimentally based on the measurement of the limiting current for the reduction of $Fe(CN)_6^{3-}$ obtained under polarographic conditions, with electrolytes at the same temperature being fed to both compartments. The results obtained (Fig. 16) agree well with the classical correlation of Norris and Streid [32], valid for a rectangular channel with laminar flow for Reynolds numbers less than 1300. For Reynolds numbers more than 1300 (circled points Fig. 16), there is deviation from the correlation of Norris and Streid [32].

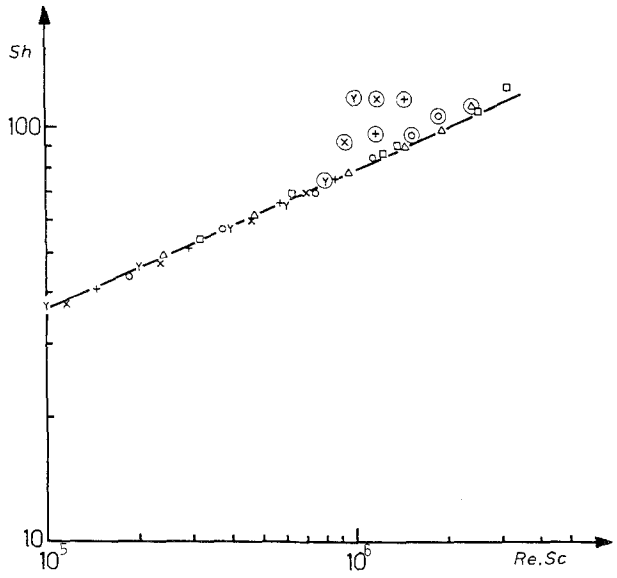

Fig. 16. Comparison of the experimental mass transfer coefficients k_d with the predicted values deduced from the Norris and Streid correlation: $Sh = 1.85\,(ReSc d_h/L)^{1/3}$. Temperature: (□) 10, (△) 20, (○) 30, (+) 40, (×) 50 and (Y) 60° C.

It should be noted that this correlation holds, even though the geometric and hydrodynamic structure of the cell does not strictly correspond to that of a simple rectangular channel, given the existence of two fluids entering into contact in the measurement zone.

It follows that: (i) a stable hydrodynamic regime is established within a very short distance following initial contact of the two fluids, and (ii) the hydrodynamic perturbations brought about by the edge of the opening in the stainless steel separator remain small and do not affect the flow near the electrodes.

4.3. *Comparison of experimental and theoretical electrochemical performance*

Equation 8, in association with global kinetic equations of the form in Equation 7, where kinetic parameters are independently determined by the procedures described in sections 4.1 and 4.2 above, constitute the basis of this comparison, shown in Figs 5 to 10. It appears that the agreement is satisfactory for the range of operating conditions investigated, which confirms the validity of the hypotheses made, particularly with respect to the effective maintenance of the thermal gradient between the two electrodes.

5. Prediction of the maximum performance of the thermopile

From the viewpoint of available electrical power, the performance of the generator depends simultaneously (*cf.* Equation 8) on two types of overpotential (concentration and activation) at the electrodes, and on the ohmic resistance, which has been shown to represent only a small fraction of R_i. In order to predict the maximum performance of the hydrodynamic system considered here, a simulation of the process was carried out for the case of infinitely rapid kinetics ($i_0 \to \infty$) and where concentration polarization phenomena constitute the principal limitation to electrical performance.

As $i_0 \to \infty$ and if the electrode exhibits Nernstian behaviour, the overpotential, η, is given by:

$$\eta = \frac{RT}{\gamma_e F} \ln\left(\frac{C_{Ac}}{C_{AS}}\frac{C_{BS}}{C_{Be}}\right) \qquad (12)$$

and for the cathodic and anodic processes, respectively, using the Nernst film model:

$$\eta_c = \frac{RT_f}{\gamma_e F} \ln\left\{\frac{1 - i(\gamma_e F k_{dc} C_{AS})^{-1}}{1 + i(\gamma_e F k_{dc} C_{BS})^{-1}(D_{Ac}/D_{Bc})}\right\}$$

and

$$\eta_a = \frac{RT_C}{\gamma_e F} \ln\left\{\frac{1 + i(\gamma_e F k_{da} C_{AS})^{-1}}{1 - i(\gamma_e F k_{da} C_{BS})^{-1}(D_{Aa}/D_{Ba}}\right\} \qquad (13)$$

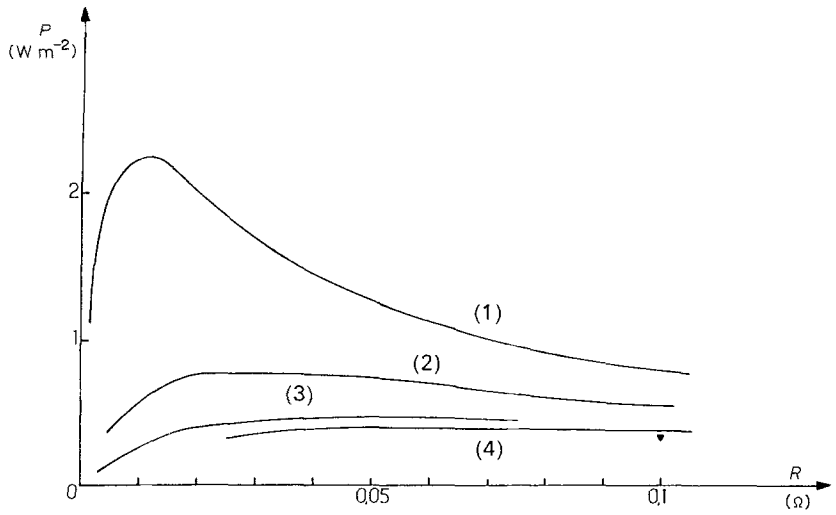

Fig. 17. Predicted values of the specific power output for $i_0 \to \infty$. Conditions: $E = 0.04\,V$, $\Delta T = 40°C$, $2\Delta = 6\,mm$, both electrolyte concentrations = 0.2 M. (——) Simulation; (▼) experimental value. (1) $i_L \to \infty$, (2) $i_L = 200\,A\,m^{-2}$, (3) $i_L = 100\,A\,m^{-2}$, (4) $i_L = 80\,A\,m^{-2}$.

The cell potential, U_C, is therefore given by the relation:

$$U_C = E - \eta_a - |\eta_c| - i\left(\frac{\Delta_c}{\gamma_c} + \frac{\Delta_a}{\gamma_a}\right) \quad (14)$$

where Δ_a and Δ_c describe the thickness of the anodic and cathodic compartments, respectively, and γ_a and γ_c are the corresponding average electrical conductivities.

The specific electrical power, p, can be calculated from the expression: $p = U_C i$, which can be expressed in the form (since $\Delta_a = \Delta_c = \Delta$ and $C_{AS} = C_{BS}$):

$$\frac{P}{i_L} = Ei^* + \frac{RT_c}{\gamma_e F} i^* \ln\left\{\frac{1 - xi^*}{1 + xi^*}\right\} + \frac{RT_f}{\gamma_e F} i^* \ln\left\{\frac{1 - i^*}{1 + i^*}\right\} - i_L i^{*2} \Delta\left(\frac{1}{\gamma_c} + \frac{1}{\gamma_a}\right) \quad (15)$$

with $i^* = i/(\gamma_e F k_{dc} C_{AS})$ = current density, expressed with respect to the cathodic limiting current density, and $x = (k_{dc}/k_{da}) = (D_c/D_a)^{2/3}$ (from the correlation of Norris and Streid).

Equation 15 shows that for fixed x, T_C and T_f, the specific power, p, depends only on i^* and i_L. The theoretical results of this simulation were used to predict the maximum electrochemical performance (when $i_{0\to\infty}$) of the thermopile. Figure 17 shows the variation of p with the resistance R of the external circuit for $(T_C - T_f) = 40°C$, $\Delta = 3\,mm$, concentration of the electroactive species 0.2 M, and for different values of the cathodic limiting current density. The curve $i_L \to \infty$ corresponds to the absence of mass transfer limitations; only ohmic overpotentials are taken into consideration. The results show that, for the temperature gradient considered, the maximum power does not exceed $2.25\,W\,m^{-2}$ (in the absence of all limitations). The experimental point reported in the figure corresponding to $u = 9 \times 10^{-2}\,m\,s^{-2}$ (with $i_L = 80\,A\,m^{-2}$) is found to be in good agreement with the model prediction. For a larger temperature gradient (corresponding to $T_f = 10°C$ and $T_C = 90°C$), the maximal power can attain $12\,W\,m^{-2}$, the thermal flux exchanged at the interface being considerably increased.

6. Conclusions

An original hydrodynamic system featuring a galvanic thermopile operating with aqueous electrolyte and utilizing two laminar flow fluid streams has been described. The experimental results concerning the influence of the principal parameters on the electrical and thermal performance of the generator show that it is possible to effectively maintain the temperature gradient between the two electrodes of the cell. The thermal short circuit at the interface between the two fluids is relatively large and, in any case, is superior to that which would be obtained under the sole effect of molecular diffusion of heat. The existence of an interfacial mixing zone resulting from the hydrodynamic perturbations arising from the contact of the two fluids explains this result.

Concerning the available electric power, the electrolyte resistance only represents a small fraction of the global resistance, which is essentially determined by the activation and concentration overpotentials at each electrode. A model based on the use of the generalized Butler-Volmer equation is found to be in excellent agreement with the experimental results (current-potential and electrical power curves) and permits the prediction of maximum performance of the thermopile under conditions of infinitely fast electrochemical kinetics. Under these optimal conditions, the specific electrical power barely exceeds $10\,W\,m^{-2}$ (for a temperature gradient of 80° C) while the thermal short circuit can attain $8000\,W\,m^{-2}$, even in the presence of a membrane separating the two compartments. The practical utilization of such generators is therefore not foreseen, given the limited performance obtained.

References

[1] W. Vielstich, 'Fuel Cells', Wiley Interscience, New York (1960) pp. 345–61.
[2] A. J. De Bethune, T. S. Light and N. Swendeman, *J. Electrochem. Soc.* **106** (1959) 616.
[3] R. Zito, *A.I.A.A. Journal* **1** (1963) 2133.
[4] D. D. Macdonald, A. C. Scott and P. Wenteek, *J. Electrochem. Soc.* **110** (1963) 1618.

[5] B. R. Sundheim, I. B. Cadoff and E. Miller, 'Thermoelectrics and Devices', Reinhold, New York (1960).
[6] T. Wartanowicz, *Adv. Energy Conversion* **4** (1964) 149.
[7] H. P. Meissner, D. C. White and G. D. Uhlrich, *ibid.* **5** (1965) 205.
[8] B. F. Markov and T. B. Kuzyakin, *Russian Chemical Reviews* **41** (1972) 250.
[9] H. Reinhold, *Z. Anorg. Allgem. Chem.* **171** (1928) 181.
[10] H. Reinhold and A. Blachny, *Z. Elektrochem.* **32** (1933) 290.
[11] C. Wagner, *Ann. Phys.* **3** (1929) 629.
[12] H. Holtan, *Koningl. Nederland akad. Wetenschap. Proc.* **1356** (1953) 498.
[13] J. L. Weininger, *J. Electrochem. Soc.* **111** (1964) 769.
[14] A. J. De Bethune, *ibid.* **107** (1960) 829.
[15] G. R. Salvi and A. J. De Bethune, *ibid.* **108** (1961) 672.
[16] J. N. Agar and W. J. Hamek, 'The structure of electrolyte solutions', Wiley & Sons, New York (1953) Chap. 13.
[17] R. Gaboriaud and P. Letellier, *J. Chim. Phys.* **3** (1975) 357.
[18] H. A. Liebhafsky, 'Thermogalvanic cell', US Patent (1959) 2 882 329.
[19] B. H. Clampitt and D. E. German, US Patent (1966) 3 253 955.
[20] B. W. Burrows, Proceedings of the 10th Intersociety Conversion Engineering conference (1975) 821.
[21] *Idem, J. Electrochem. Soc.* **123** (1976) 154.
[22] I. M. Kolthoff and E. A. Pearson, 'Stability of Potassium Ferrocyanide solutions. Industrial and Engineering Chemistry', **3** 4 (1971) 381.
[23] J. P. Bourne, P. Dell'ava, O. Dossenbach and T. Post, *J. Chem. Eng. Data* **30** (1985) 160.
[24] N. B. Vargaftik, 'Tables of the Thermophysical Properties of liquids and gases', 2nd edition, Hemisphere Publishing, New York (1975).
[25] D. Dobos, 'Electrochemical Data', Elsevier Scientific, New York (1975).
[26] Y. S. Touloukian, P. E. Laley and S. C. Saxena, 'Thermophysical Properties of Matter', Vol. 3, Liley (1970).
[27] E. W. Washburn, 'International Critical Tables of Numeric Data, Physics, Chemistry and Technology', Vol. 5, McGraw-Hill, New York (1929).
[28] A. L. Horvath, 'Handbook of Aqueous Solutions', Wiley & Sons, New York (1985).
[29] P. Bourret, private communication (1982).
[30] J. M. Hornut, 'Analyse Experimentale et théorique d'une pile thermogalvanique ou de concentration à convection forcée de deux liquides: Transfert de chaleur ou de matière à l'interface', Ph. D. Thesis INPL-Nancy (1987).
[31] K. J. Vetter, 'Electrochemical Kinetics: Theoretical and Experimental Aspects', Academic Press, New York (1967).
[32] R. H. Norris and P. D. Streid, *Trans. ASME* **62** (1940) 525.